Modification of Electro-Fenton Process with Granular Activated Carbon for Phenol Degradation – Optimization by Response Surface Methodology

Hind H. Thwaini[1*], Rasha H. Salman[1]

[1] Department of Chemical Engineering, College of Engineering, University of Baghdad, Baghdad, Iraq
* Corresponding author's e-mail: hind.abd2107m@coeng.uobaghdad.edu.iq

ABSTRACT

As a result of rapid industrialization and population development, toxic chemicals have been introduced into water systems in recent decades. Because of its excellent efficiency and simple design, the three-dimensional (3D) electro-Fenton method has been used for the treatment of wastewater. The goal of the current study is to explore the efficiency of phenol removal by the 3D electro-Fenton process, which is one of the advanced oxidation processes (AOPs). In the present work, the effect of the addition of granular activated carbon (GAC) particles to the electro-Fenton system as the third electrode would be investigated in the presence of graphite as the anode and nickel foam as the cathode, which is the source of electro-generated hydrogen peroxide (H_2O_2). The influence of operation parameters (current density, electrolysis time, and GAC) on catalytic performance will be studied, which will be adjusted by the response surface methodology (RSM). The pH was adjusted to 3, and the airflow was set to 10 L/h. According to the results the nickel foam was an excellent cathode material choice. The best conditions for phenol elimination were at current density of 3.56 mA/cm², $FeSO_4.7H_2O$ dosage of 0.1 mM, GAC of 30 g, and a time of 3 h to attain the removal rates of phenol and chemical oxygen demand (COD) of 98.79% and 93.01%, respectively. The results showed that time had a higher effect on the phenol and COD removal efficiency, while the impact of current density was lower. The model equation's high R^2 value (97.90%) demonstrates its suitability.

Keywords: electro-fenton; nickel foam; GAC; phenol degradation; hydroxyl radical; response surface methodology.

INTRODUCTION

Phenol and related derivatives can be found in effluents from various industries, including petroleum refineries, petrochemical plants, coking operations, pharmaceutical manufacturing, and the phenolic resins industries [Ho, 2022]. The United States Environmental Protection Agency (USEPA) and Canada's National Pollutant Release Inventory (NPRI) both classify phenol as a priority pollutant [Mohd, 2022]. Phenolic compounds can be detected in amounts of 800-2000 mg/L in industrial effluents where phenol is present as an intermediary. Phenol leakage into the environment risks human health and destroys the environment [Abd Gami et al., 2014]. Phenol is a colorless crystalline material at room temperature that possesses hydroscopic characteristics in water and marginally in organic solvents, making it easily spilled or leaked into surface water or groundwater sources [Atsdr, 2008]. Heavy metals and phenols were produced by industry and accumulated in the environment, destroying ecosystems [Khalid and Salman, 2019]. Water quality has a significant impact on the health of humans and all other living things. As a result, surface and groundwater contamination by dangerous or persistent chemicals has become a considerable concern [Adil Sabbar, 2019]. Many studies have been conducted to reduce and even eliminate some undesirable compounds from water using various approaches such as coagulation, adsorption, oxidation, biological processing, and electrochemistry [Al-Rubaiey, 2022]. Toxic chemicals have been added to water systems in recent decades as a result of increasing industrialization

and population growth [Abbas et al., 2016]. The electro-Fenton is environmentally friendly and does not create secondary pollutants because the power used is clean and pollution-free [Abbas and Abbas, 2022]. It is based on the electrochemical production of H_2O_2 Eq. 1 over an extended period of time at a suitable cathode by the reduction of dissolved oxygen or air with the addition of an iron catalyst Eq. 2 to the treated solution, and the Fe^{2+} ions can be created by reducing the Fe^{3+} at the cathode Eq. 3 [Bury et al., 2021]. Through the use of a variety of chemical intermediates, phenol is transformed into CO_2 and H_2O, which are relatively safe byproducts [Oturan et al., 2021].

$$O_2 + 2H^+ + 2e^- \rightarrow H_2O_2 \qquad (1)$$

$$Fe^{2+} + H_2O_2 \rightarrow Fe^{3+} + OH^- + OH^\cdot \qquad (2)$$

$$Fe^{3+} + e^- \rightarrow Fe^{2+} \qquad (3)$$
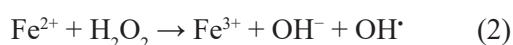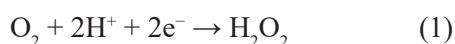
A promising alternative technique, modified electro-Fenton, for significantly increasing the working electrode's specific surface area has recently proposed, and it has been successfully used to remove phenolic compounds. This procedure uses a 3D electrode technique that contains carbon particles [Sun et al., 2017]. The 3D electrode reactor, a revolutionary advanced oxidation method, has gained attention for successfully degrading materials in the advanced oxidation processes because of its high effectiveness, simplicity of use, and compatibility with the environment among other processes [Zhang et al., 2020]. In terms of current efficiency, energy consumption (EC), and pollutant removal efficiency, the 3D electrode technology is superior to two-dimensional electrode technology [Zheng et al., 2019]. As a result, adding a granular electrode to the classic electrochemical unit is regarded as a good enhancement for increasing the activity and current density of the electrochemical technique [Yan et al., 2011]. In the electro-Fenton method that used granular electrodes (3D) systems, the gap between the granular electrodes was shorter, allowing for faster electron transport and increased removal efficiency [Yang and Tang, 2018]. A big effective contact area and a large number of micro-electrolysis cells are provided by the 3D electrode system, which uses GAC. The electric chemical reaction expands onto the surface of each particle electrode as well as the primary electrode, where it initially reacted [Zhang et al., 2013]. The granular electrode has a large specific surface area, excellent chemical stability, and exceptional

conductivity, making it suitable for use as a 3D electrode [Norra and Radjenovic, 2021].

On the other hand, the Fenton reagent generation process greatly benefits from an increase in the electrode surface area. The formation of hydroxyl radicals can be increased by enhancing the cathode's conductivity and specific surface, which eventually improves the removal of contaminants [Haji Ali et al., 2021]. In addition to its superior advantage due to its porous structure and high conductivity, nickel foam was a practical substitute for the creation of H_2O_2, where its accumulation at the nickel foam cathode was five times larger than that of the graphite electrode. Faster electron transfers in this electrode produce O_2 on its surface and increase the amount of H_2O_2 in the system, which increases the amount of $OH^\cdot$ formation [Bocos et al., 2016; Hu et al., 2019].

The present study was planned to obtain the best reaction condition for phenol oxidation. In addition, the influence of GAC addition on electro-Fenton reaction performance was examined by applying these particles as the third electrode in an electrolytic cell with nickel foam as the cathode and graphite as the anode. The enhanced degradation of phenol was due to the combined effect of GAC and oxidation reactions of nickel foam.

EXPERIMENTAL WORK

Chemicals

The chemicals used in this study were all analytical grade and didn't need to be further purified. Phenol crystals (with 99.5% purity, Alpha Chemical Reagent Company, India), sodium sulfates Na_2SO_4 (with 99.0%, purity SDFCL), ferrous sulfate heptahydrate $FeSO_4.7H_2O$ (CDH, Company), and sulfuric acid (with 98% purity, Sigma-Aldrich) were the utilized chemicals. Nickel foam was purchased from (Xiamen Top New Energy Technology, China), GAC from (Sigma-Aldrich), and In order to create the aqueous solutions, deionized water was employed.

Experimental methods

A batch experiment was carried out in a 1.0 L glass reactor filled with an aqueous solution containing 1.0 L with 150 mg/L of phenol. A perspex cover with a thickness of 10 mm was employed, with two holes to secure the electrodes and three

holes for inserting the thermometer, airflow source, and sample extraction. The cathode was a nickel foam plate (130×50×10 mm), and the anode was a graphite plate (130×50×5 mm) with a gap of 3 cm between the electrodes. Nickel foam was washed to eliminate any oxides on the surface with de-ionized water and 0.1 M H_2SO_4. Before starting any run, the solution was aerated with air with an electromagnetic air pump ACO-001 China, at a rate of 10 L/h for 20 minutes and remained that way until the experiment was completed. Air is circulated through the solution using a glass tube connected to the diffuser. To provide constant current density, a digital (DC) power supply (0–30 V, 0–5 A) of the type (UNI-T, UTP3315PE) was used. A catalytic amount of 0.1 mM was added to give Fe^{2+} for the reaction, and a necessary amount of Na_2SO_4 (0.01 M) was supplied to support the electrolyte and increase electrolyte conductivity. The pH of the solution was set to 3 by adding 0.1 M H_2SO_4 or 0.1 M NaOH.

GAC is sieved to a particle size of over 1.5 mm in diameter using medium-size sieve No. 16 (1.18mm) and then washed with deionized water to remove impurity compounds. Finally, the particles were dried in an oven at 105 °C for 6h before being utilized as the third electrode in the reactor [Roddaeng et al., 2018]. The specific surface area and total pore volume were determined using the BET method, based on nitrogen adsorption and desorption isotherms which was evaluated using Brunauer-Emmett-Teller (Horibe, SA-9600 model, USA), the surface area was 1023 m^2/g,

and the pore volume was 0.20104 m^3/g. Samples were withdrawn and filtered through a 0.45 µm filter paper, and the COD and phenol concentrations were determined by the (Lovibond, RD125, Germany) and (Spectrometers, UV-9200, UK) respectively. A schematic drawing of the 3D electro-Fenton system is shown in Figure 1.

The efficiency of phenol removal was evaluated by Eq. 4 [Abbas and Abbas, 2019].

$$\text{Phenol } Re\% = ((C_0 - C_f)/C_0) \times 100 \qquad (4)$$

where: C_0 – the initial phenol concentration (mg/L), C_f – the final phenol concentration (mg/L), phenol $Re\%$ – the removal efficiency of phenol. Energy consumption (EC) – calculates how much energy is expended during the digestion of one kilogram of phenol. Eq. 5 can be used to estimate the EC in kWh/kg phenol.

$$EC = (I \times voltage \times t \times 1000) / (\Delta \text{ phenol} \times V) \quad (5)$$

where: I – the operating current intensity, V – the volume of the solution, t – the time, Δ phenol – phenol degradation in solution during experimentation [Fahem and Abbar, 2020; Gümüş and Akbal, 2016].

Electrode analysis

Graphite and nickel foam were used as the anode and cathode materials. The structural properties of these electrodes were determined using an X-ray diffractometer (Shimadzu, XRD 6000
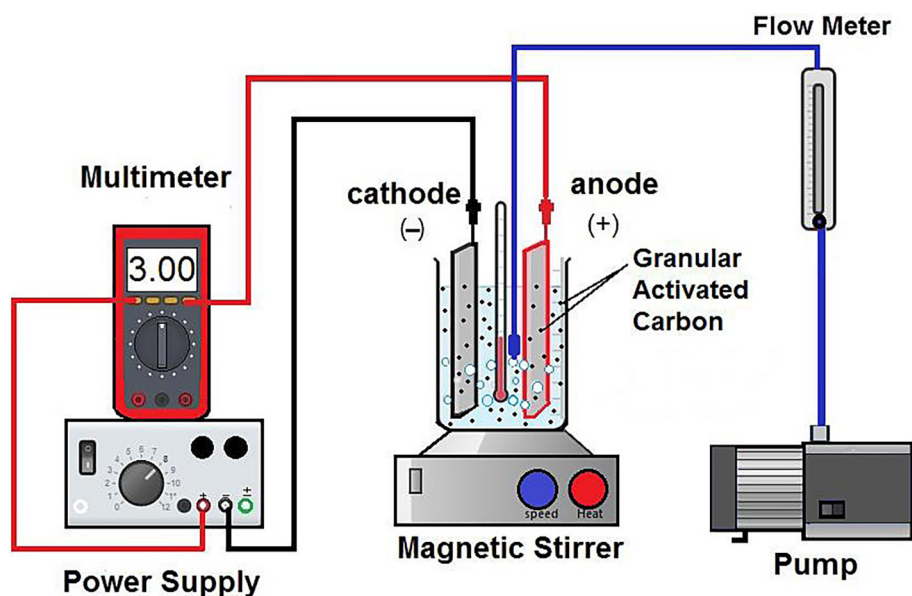
Figure 1. A diagram of the 3D electro-fenton system

model, Japan). The following were the device's characteristics: The X-ray tube was operated at a scan speed of 5 degrees per minute with a voltage of 40 kV and a current of 30 mA, with CuKα radiation as the X-ray source. Figure 2 depicts the XRD patterns of graphite and nickel foam. The XRD pattern of graphite exhibits a sharp and tight peak at $2\theta = 26.5°$, which corresponds to the diffraction line C (002). This indicates the existence of sole carbon [Siburian et al., 2018], whereas the Ni foam peaks are located at approximately $2\theta = 44.5°$, $51.9°$, and $76.4°$ [Hu et al., 2019]. The surfaces of the electrodes and GAC were investigated with a scanning electron microscope (SEM) (FEI Company, Netherlands), with Inspect S50 at 25 kV and 100 microamperes. SEM images of graphite, nickel foam, and GAC as shown in Figure 3. The SEM photos of graphite revealed a semi-porous
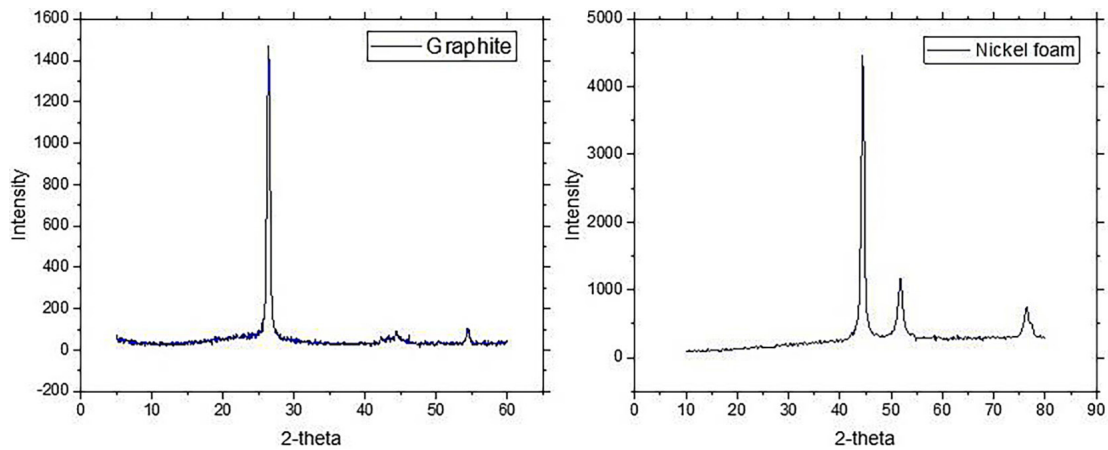
Figure 2. XRD pattern for graphite, and nickel foam
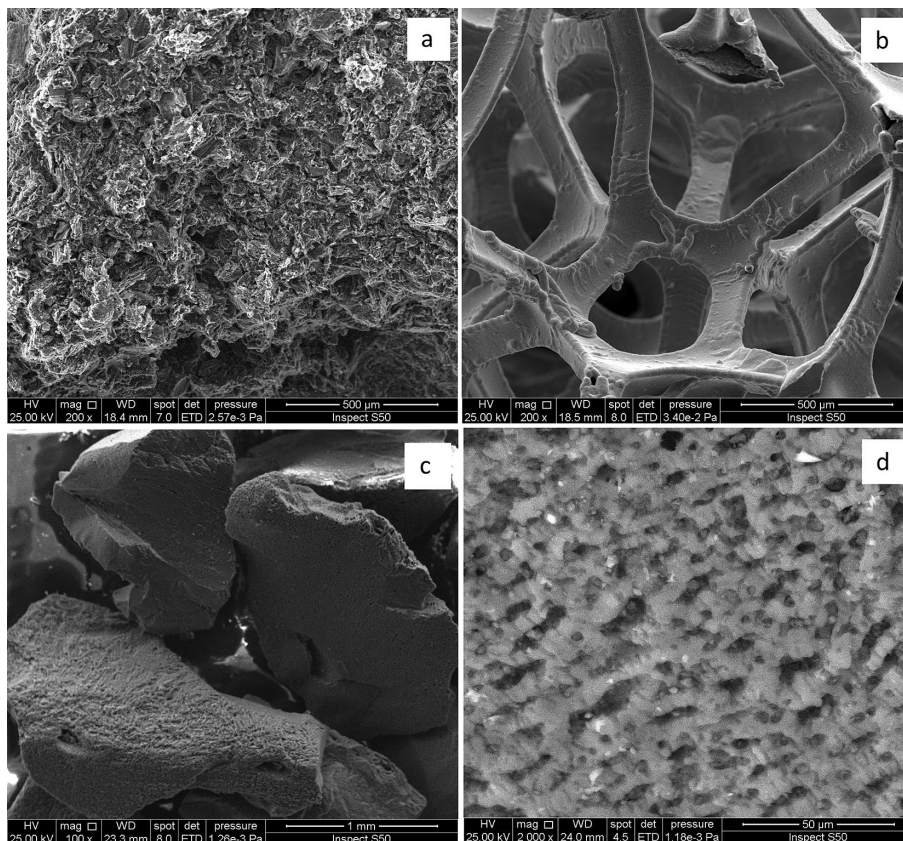
Figure 3. SEM of (a) graphite (with zoom of 500 µm), (b) nickel foam (with zoom of 500 µm), (c) GAC (with zoom of 1 mm), and (d) GAC (with zoom of 50 µm)

and flaky surface, but the nickel foam exhibited a characteristic porous structure with a high surface area. The porous structure of the surface can be seen by the SEM of GAC. The surface of nickel foam before and after the reaction is depicted in Figures 8a and b. The EDX (Energy Dispersive X-ray spectroscopy) measurements in Figure 4 from Bruker Company/Germany, XFlash-6110, 25 KV, and 100 A demonstrate pure carbon due to the graphite and GAC, while Ni, C, O, and N are due to the Ni foam.

Experimental design

The Box-Behnken experimental design (BBD) was utilized, where three levels and three-factor parameters that controlled phenol elimination were tested and verified in the present study [Ghjair and Abbar, 2022]. The process variables were electrolysis time (X1), GAC (X2), and current density (X3), with the response being phenol elimination efficiency. The numbers represent the scales of the process variables: (-1) is the low level, (0) is the middle point, and (1) is the high level. The Minitab-18 program was used to examine the phenol removal efficiency (Re %) results.

Table 1 displays the experimental parameters and their levels, while Table 2 displays the trials that would be carried out according to the BBD in coded and real values.

The empirical quadratic polynomial model as shown in Eq. 6 would represent the mathematical relationship between independent factors and response [Umar et al., 2018].

$$Y = \alpha_0 + \sum \alpha_i x_i + \sum \alpha_{ii} x^2_i + \sum \alpha_{ij} x_i x_j \quad (6)$$

where: Y – represents the response (Re%), i and j are the index numbers for independent variables, a_0 – the intercept term, $x1$, $x2$ … xk – the process variables (independent variables) in coded form, a_i – the first-order (linear) main effect, a_{ii} – second-order main effect, and aij is the interaction effect. Analysis of variance was performed.

RESULTS AND DISCUSSION

Statistical analysis

Fifteen batch runs at various process factor combinations were performed in order to
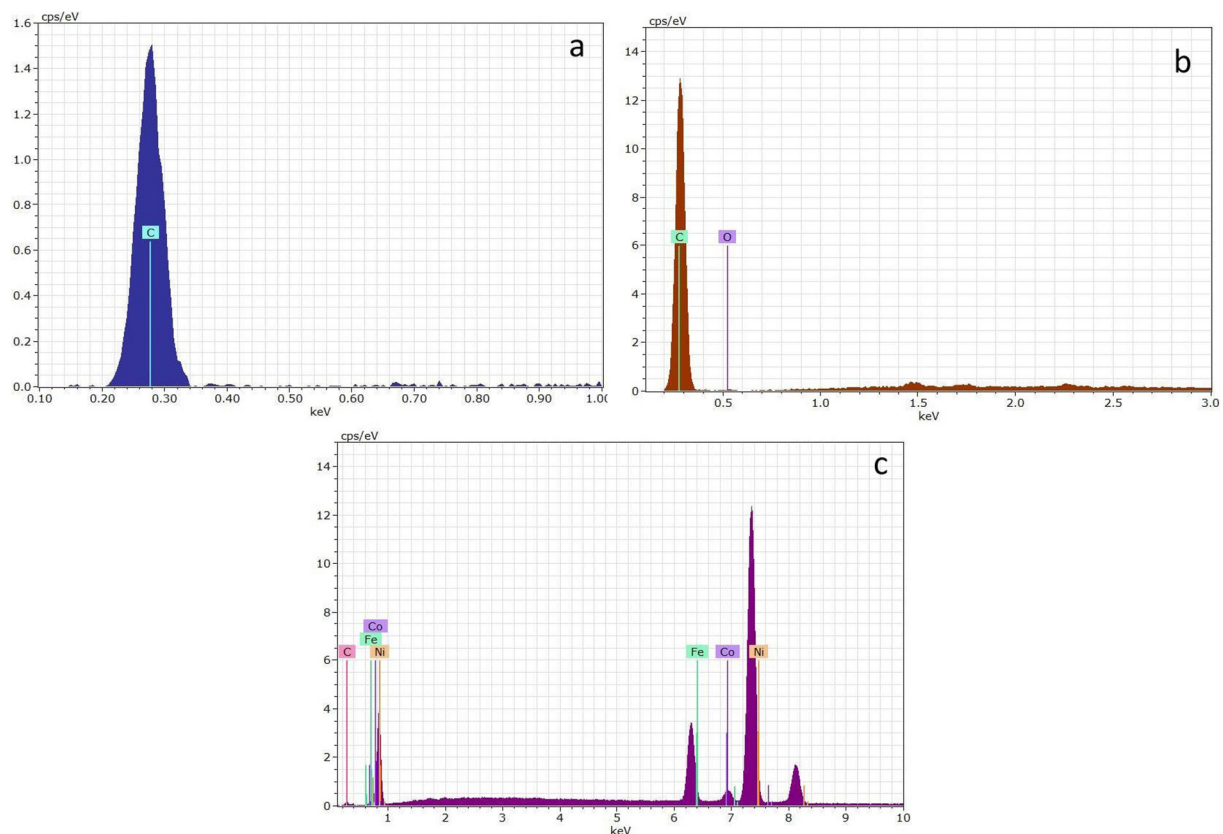
Figure 4. EDX of (a) Graphite, (b) GAC, and (c) Nickel foam

Table 1. Process factors and their levels on phenol elimination

Independent variable	Signs	Unit	Low (-1)	Center (0)	High (1)
Time	X1	h	1	2	3
GAC	X2	g	10	20	30
Current density	X3	mA/cm^2	3	4	5

Table 2. Box-Behnken design for phenol removal

Run	Bk.	Coded value			Real value		
		x1	*x2*	*x3*	Time (h), X1	GAC (g), X2	Current density (mA/cm^2), X3
1	1	0	0	0	2	20	4
2	1	0	-1	-1	2	10	3
3	1	-1	0	1	1	20	5
4	1	0	1	1	2	30	5
5	1	0	1	-1	2	30	3
6	1	0	0	0	2	20	4
7	1	1	-1	0	3	10	4
8	1	1	0	-1	3	20	3
9	1	-1	-1	0	1	10	4
10	1	0	-1	1	2	10	5
11	1	1	1	0	3	30	4
12	1	-1	0	-1	1	20	3
13	1	0	0	0	2	20	4
14	1	-1	1	0	1	30	4
15	1	1	0	1	3	20	5

optimize and investigate the combined effects of the independent parameters on phenol removal efficiency. Table 3 displays the experimental and predicted phenol removal efficiency (*Re*%) and energy consumption values. The Minitab-18 was used to evaluate the removal efficiency results and attain a quadratic model of phenol removal efficiency in terms of un-coded (real) process parameters, as shown in Eq. 7.

$$\text{Phenol } Re\% = 27.9 - 1.88\, X1 + 1.784\, X2 + 10.56\, X3 + 3.49\, (X1)^2 - 0.0159\, (X2)^2 - 0.85\, (X3)^2 - 0.056\, (X1X2) - 0.63(X1X3) - 0.085\,(X2X3) \quad (7)$$

The results showed that the efficiency of phenol removal was in the range of 68.3419–98.1% and the specific energy consumption was in the range of 7.8128–31.2989 kWh/kg phenol. Time has a greater impact on phenol elimination, as shown by the comparison of runs 14 and 11. At a constant GAC dosage of 30 g and current density of 4 mA/cm^2, phenol removal increased from 74.8094% to 98.1%, making a difference of 23.2906% as time increased from 1 to 3 h. Also, based on this comparison, it is clear that

increasing the electrolysis time from 1 to 3 h led to an increase in EC from 10.8943 to 27.9051 kWh/kg phenol. Phenol removal efficiency increased from 83.8756 to 98.1% with a difference of 14.2244%, as shown in the results of runs 7 and 11, by increasing the GAC dosage from 10 to 30 g. This indicates that increasing the dosage of GAC had a second influence on phenol removal. Also, by comparing the values of EC, it is obvious that by increasing the GAC dosage from 10 to 30 g, the EC decreased from 30.4021 to 27.9051 kWh/kg phenol due to an increase in the removal of phenol by increasing the GAC dosage. Additionally, as shown in runs 15 and 8, when the current density increased from 3 to 5 mA/cm^2, an increase in phenol removal from 90.9987% to 94.4329% with a 3.4342% difference was attained, which clarifies the small effect of current density on the phenol removal efficiency. Also, based on this comparison, it is clear that increasing the current density from 3 to 5 mA/cm^2 led to an increase in EC from 12.3416 to 18.4098 kWh/kg phenol due to a decrease in the phenol removal.

Analysis of variance (ANOVA)

An ANOVA analysis was performed based on the response surface model, as shown in Table 4. The following terms were examined in this table. The percentage of contribution (Cr.%), the degree of freedom (DF), the sum of the square (Seq. SS), the adjusted sum of the square (Adj. SS), and the adjusted mean of the square (Adj. MS). A P-value and F-value of (0.001) and (25.94) were found, indicating that the regression model is very significant [Issa and Salman, 2023]. The model's multiple correlation coefficient can be used to predict the effectiveness of phenol removal in the

Table 3. Experimental results for phenol removal efficiency

Run	Bk.	Time, h	GAC, g	Current density, mA/cm^2	Actual Phenol Re%	Predicted Phenol Re%	E, volt	EC, (kWh/kg phenol)
1	1	2	20	4	80.9987	81.8737	5.05	20.9
2	1	2	10	3	71.2356	70.8640	4.8	23.8195
3	1	1	20	5	75.8580	77.4492	5.4	15.0815
4	1	2	30	5	85.9233	86.2949	5.8	28.3508
5	1	2	30	3	85.4298	86.4884	4.9	14.5304
6	1	2	20	4	80.9990	81.8737	5.03	20.6998
7	1	3	10	4	83.8756	85.8384	5.1	30.4021
8	1	3	20	3	94.4329	92.8417	4.575	18.4098
9	1	1	10	4	68.3419	67.8092	4.4	10.7303
10	1	2	10	5	75.1462	74.0877	5.6	31.2989
11	1	3	30	4	98.1000	98.6327	5.475	27.9051
12	1	1	20	3	73.7675	74.6717	4.55	7.8128
13	1	2	20	4	83.6233	81.8737	5.04	20.09
14	1	1	30	4	74.8094	72.8466	4.89	10.8943
15	1	3	20	5	90.9987	90.0945	5.524	12.3416

Table 4. Variance analysis for phenol reduction

Source	DF	Seq. SS	Contr. %	Adj. SS	Adj. MS	F-value	P-value
Model	9	1030.92	97.90%	1030.92	114.547	25.94	0.001
Linear	3	963.62	91.51%	963.62	321.208	72.73	0.000
Time, X1	1	571.73	54.30%	571.73	571.734	129.46	0.000
GAC, X2	1	387.30	36.78%	387.30	387.299	87.70	0.000
Current density, X3	1	4.59	0.44%	4.59	4.591	1.04	0.355
Square	3	61.52	5.84%	61.52	20.508	4.64	0.066
X1X2	1	50.25	4.77%	45.08	45.084	10.21	0.024
X2X2	1	8.59	0.82%	9.29	9.290	2.10	0.207
X3X3	1	2.69	0.26%	2.69	2.691	0.61	0.470
2-Way interaction	3	5.77	0.55%	5.77	1.923	0.44	0.737
X1X2	1	1.26	0.12%	1.26	1.258	0.28	0.616
X1X3	1	1.59	0.15%	1.59	1.594	0.36	0.574
X2X3	1	2.92	0.28%	2.92	2.919	0.66	0.453
Error	5	22.08	2.10%	22.08	4.416		
Lack-of-Fit	3	17.49	1.66%	17.49	5.830	2.54	0.295
Pure Error	2	4.59	0.44%	4.59	2.296	-	-
Total	14	1053.00	100.00%	-	-	-	-
Model summary	S	R^2	R^2 (adj.)	Press	R^2 (pred.)	-	-
	2.10147	97.90%	94.13%	290.155	72.44%	-	-

3D electro-Fenton reactor, as evidenced by the high value of R^2, which was 97.90%, showing that the model was statistically significant. Electrolysis time had the highest significant effect on the phenol removal efficiency with a high F-value = 25.94 and Cr.% of 54.30, the GAC dosage had lower Cr.% 36.78, and finally the current density had the lowest effect on the phenol removal efficiency with Cr.% of 0.44.

Effect of parameters

The interactive impacts of the selected parameters and their effects on the response were shown graphically in RSM, and this was utilized to analyze the result. To investigate the interactions between operating parameters and phenol removal more thoroughly, contour and three-dimensional plots were illustrated, as shown in Figures 5a, and b, respectively. Figures 5a and b show the effect of time on phenol removal efficiency over a range of current densities (3–5 mM/cm^2) under a constant GAC dosage of 20 g and a time of 3 h. According to the contour plot in Figure 5a, phenol removal efficiency greater than 90% is obtained only within a range of current density (3-5 mM/cm^2) within an electrolysis time of 2.8–3 h. From the surface plot, it is clear that at a time of 1 h, a noticeable decrease in phenol removal efficiency occurred, while at a higher value of time (3 h), the efficiency of phenol removal increased linearly with a current density of 3–5 mM/cm^2, and this result is in agreement with a previous study [Davarnejad and Sahraei, 2016]. As shown in Figure 5b, the efficiency of phenol removal increases gradually as the current density increases from 3–5 mA/cm^2. The electro-Fenton process removes more phenol when the current density is higher,

which may be due to the fact that current causes the reduction of oxygen on the cathode surface that produces H_2O_2. Accordingly, increasing the current density would cause more hydroxyl radicals because H_2O_2 and ferrous ions would react more frequently [He and Zhou, 2017]. From these experimental results, it is evident that the optimal current density was 3.56566 mA/cm^2 for phenol degradation. The removal efficiency of phenol increased to some extent with an increase in the current density, which is proportional to the number of charges produced in electrochemical reactions. Theoretically, increasing the current density could accelerate the rate of electrolysis [Nidheesh et al., 2023]. The findings indicate that reaction time has a positive impact on the progress of the electro-Fenton process for a period of time.

The material of the particle electrode in a 3D particle electrode system is a significant variable impacting system effectiveness and cost [Zhang et al., 2013]. The removal rate of pollutants improved when utilizing the 3D electrochemical process because, in addition to particulate electrode polarization, these particles (adsorbents) can serve as reactive sites for pollutant adsorption or even catalytic reactions due to their high specific surface areas [Dao et al., 2020].

Figures 6 a and b depict the impact of time on the phenol removal efficiency with GAC dosage variation and a constant current density equal to 4 mA/cm^2. The efficiency increased linearly with time and exponentially with GAC dosage, and the contour plot shows a small area of high removal efficiency can be obtained at a GAC dosage of 22–30 g and the time between (2.8 and 3h). The 3D response surface shows that more than 95% of the phenol removal value was attained at GAC equal to 30 g [Yang et al., 2012]. Electrolysis time
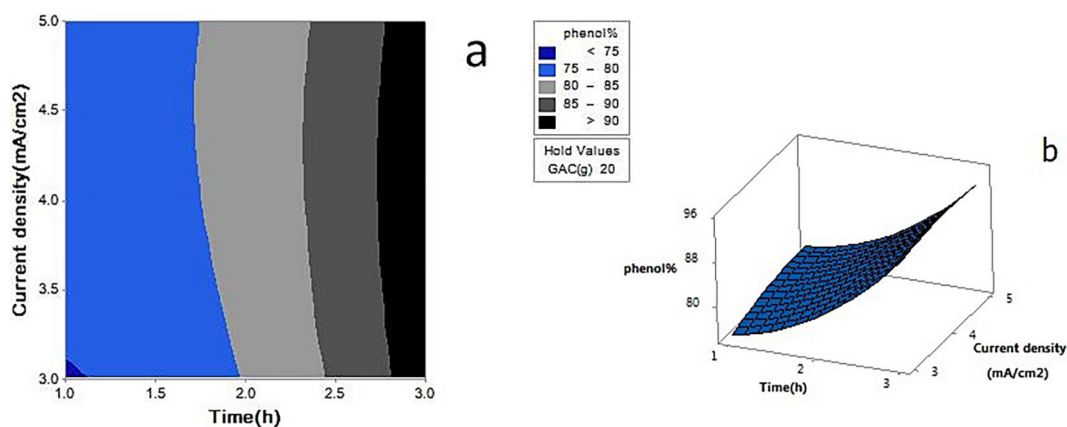
Figure 5. (a) Contour plot (b) 3D plot for phenol removal *Re*% at GAC hold value = 20 g
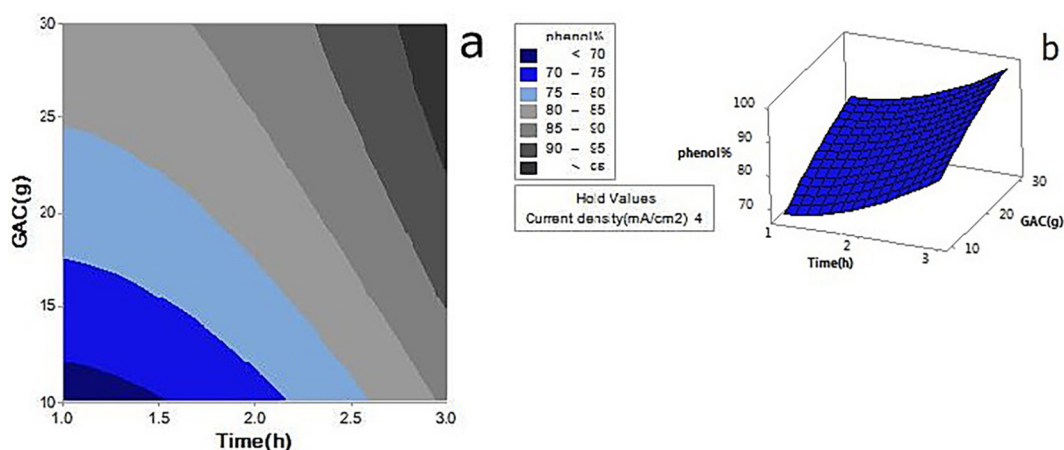
Figure 6. (a) Contour plot (b) 3D plot for phenol removal *Re*% at current density hold value = 4 mA/cm^2

is an essential factor, and it influences the generation rate of active radicals while reducing pollutants [Ibrahim and Salman, 2022]. The increase in removal efficiency when using particle electrodes is mostly due to the presence of chains of microelectrodes in the electric field. The effectiveness of both direct and indirect oxidation processes is improved by these microelectrodes' increased production of hydroxyl radicals [Singh et al., 2019].

Figures 7a and b show the relation between current density and GAC dosage on the phenol removal efficiency at a constant electrolysis time of 2 h. The phenol removal efficiency increased as the current density increased from 3.5 to 4.5. According to these results, the best current density for phenol degradation was 3.56566 mA/cm^2. The phenol removal effectiveness increased to some level as current density increased, which is related to the number of charges created in electrochemical reactions. In theory, boosting the current density could hasten the rate of electrolysis. Therefore, too high current density was not recommended.

Fockedey and Lierde also reported that a simple increase in current intensity would lead to a large decrease in removal efficiency in phenol electrooxidation by using three-dimensional electrodes [Fockedey and Lierde, 2002].

Yang et al. 2012, used GAC for the degradation of phenol in a 3D electro-Fenton system with two graphite electrodes as anode and cathode with 333 g/l of GAC as the third electrode, and 93% of phenol removal efficiency in 3 h was attained. In this study, the maximum dosage of GAC was 30 g/l for eliminating the phenol to 98.1% in 3h which clarifies the high efficiency of nickel foam as cathode in the present system in comparison with graphite [Yang et al., 2012].

The optimization and confirmation test

Outlining the optimal values of parameters to maximize phenol removal efficiency is the primary objective of the optimization. To achieve the highest phenol removal efficiency by the
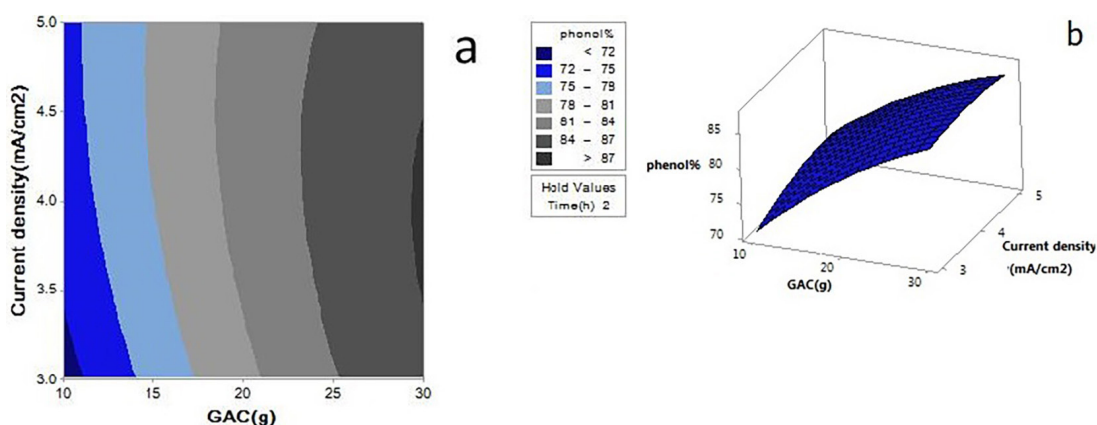
Figure 7. (a) Contour plot (b) 3D plot for phenol *Re*% at time hold value = 2h

3D electro-Fenton technique, the ideal aim in terms of phenol removal efficiency was defined as "maximizing". The results of the optimal values are presented in Table 5. Two confirmation experiments were conducted under optimal values of operating variables to obtain the highest value of phenol removal efficiency and the corresponding value of COD. The average phenol removal efficiency attained at optimum conditions was 98.805%, as shown in Table 6, and the COD value at these conditions was 91.46% with consumed energy of 25.21 kWh/kg phenol. Comparing these results with the 2D electro-Fenton system showed that at the same condition, the phenol and COD removal efficiencies were 71.65% and 68.34%, respectively, which clarifies the high efficiency of the 3D electro-Fenton system.

Nickel foam analysis

The increase in electrode surface area, is critical in the synthesis of the Fenton reagent. The formation of hydroxyl radicals can be increased by boosting the conductivity and specific surface of the cathode, which ultimately leads to an improvement in the elimination of pollutants [Bocos et al., 2016]. The previous SEM of pure Ni foam in Figure 3b retained its three-dimensional porous structure. Phenol was successfully eliminated in the presence of Ni foam; a chemical reaction generated a significant modification in the surface form. In a micro scale photograph, the original Ni foam had a smooth surface as shown in Figure 8a. Figure 8b showed the flaws on the top of the Ni foam which indicated that nickel leached during the process, which is consistent with the improved removal efficiency [Wan et al., 2017].

GAC analysis

The SEM image in Figure 9a shows the GAC before the reaction has high porosity with large pores formed between interconnected structures. The existence of cavities in the GAC structure is

Table 5. Optimal performance of system variables for the maximum removal of phenol

Run	Time, h	GAC, g	CD, mA/cm^2	E, Volt	EC, kWh/kg phenol	Actual phenol Re%	Average
1	3	30	3.56	5.17	25.236	98.6	98.805
2	3	30	3.56	5.15	25.179	99.01	

Table 6. Confirmation experiments of phenol removal

Solution of parameters			Multiple response prediction			
Time, h	GAC, g	Current density, mA/cm^2	Phenol% fit	SE fit	95% CI	95% PI
3	30	3.56566	98.7878	1.91	(93.87; 103.71)	(91.48; 106.10)
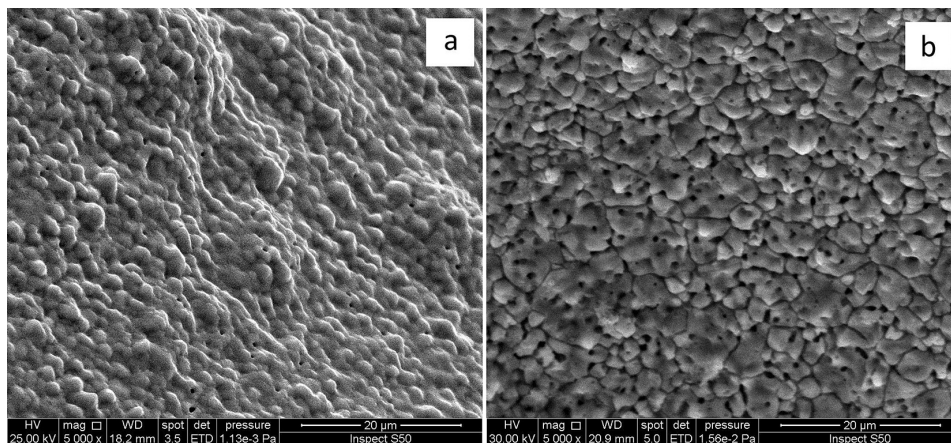
Figure 8. SEM of (a) nickel foam before reaction (with zoom of 20 μm)
(b) nickel foam after reaction (with zoom of 20 μm)
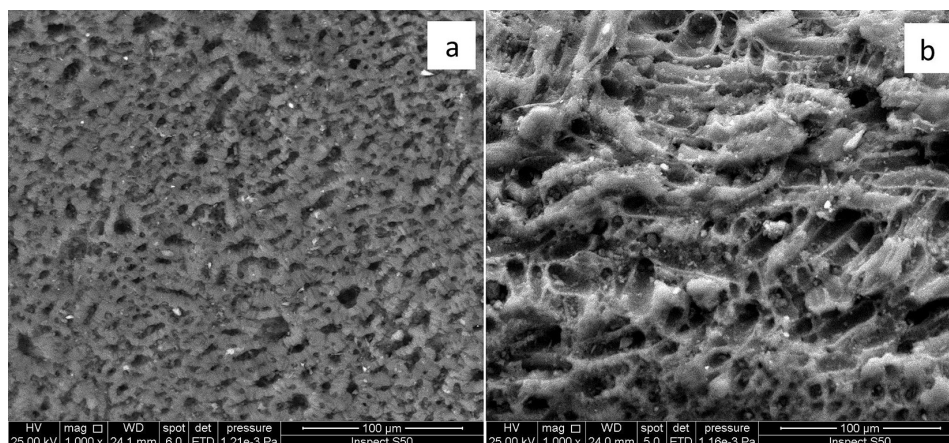
Figure 9. SEM of (a) GAC before reaction (with zoom of 100 μm)
(b) GAC after reaction (with zoom of 100 μm)

advantageous for the adsorption process because it allows phenol molecules to penetrate the adsorbent [Lütke et al., 2019; Li et al., 2021]. A clear difference in the GAC structure after and before the reaction is shown in Figure 9 where it is evident that the pore collapse resulting in blockages which reduced the surface area from 1023 to 699 m^2/g and the pore volume from 0.20104 to 0.1327 m^3/g after the reaction.

CONCLUSION

This research was carried out to remove phenol from aqueous solutions by modifying the 2D electro-Fenton process with granular activated carbon to predict a 3D electro-Fenton system with high enhancement. A three-level Box-Behnken design with three variables, current density, electrolysis time, and GAC dosage, was utilized to simulate and optimize phenol removal. Nickel foam was employed as the cathode to increase phenol elimination effectiveness and provide a large surface area. The P and F values demonstrated that the overall acceptability model was significant and that this model gave a valid R^2 value equal to 97.90%, which verified the model's validity. The biggest phenol elimination efficiency was achieved at 30 g of GAC dosage, 3 h of electrolysis, and 3.56566 mA/cm^2 of current density, the COD was 93.01%, and the phenol removal efficiency was about 98.8% under these ideal conditions. According to the ANOVA findings, the time has the biggest impact on the effectiveness of the procedure, and nickel foam was an efficient electrode. From an economic and operational standpoint, the 3D electro-Fenton process with an anode made of graphite and a cathode made of nickel foam with GAC as a third electrode is a very effective treatment method, as it achieves an excellent removal rate and lower energy and material consumptions.

REFERENCES

1. Abbas, A.S., Hafiz, M.H., Salman, R.H. 2016. Indirect Electrochemical Oxidation of Phenol Using Rotating Cylinder Reactor. Iraqi Journal of Chemical and Petroleum Engineering. 17(4), 43–55.

2. Abbas, R.N., Abbas, A.S. 2022. Kinetics and Energetic Parameters Study of Phenol Removal from Aqueous Solution by Electro-Fenton Advanced Oxidation Using Modified Electrodes with PbO2 and Graphene. Iraqi Journal of Chemical and Petroleum Engineering, 23(2), 1–8.

3. Abbas, Z.I., Abbas, A.S. 2019. Oxidative degradation of phenolic wastewater by electro-fenton process using MnO2-graphite electrode. Journal of Environmental Chemical Engineering, 7(3).

4. Abd Gami, A., Yunus Shukor, M., Abdul Khalil, K., Aini Dahalan, F., Khalid, A., Aqlima Ahmad, S. 2014. Phenol and Phenolic Compounds Toxicity, 2(1), 11-23.

5. Adil Sabbar, H. 2019. Adsorption of Phenol from Aqueous Solution using Paper Waste. Iraqi Journal of Chemical and Petroleum Engineering, 20(1), 23–29.

6. Al-Rubaiey, N. 2022. A trends in Ozone Treatment of Wastewater: a Review. Iraqi Journal of Oil and Gas Research (IJOGR), 2(1), 55–64.

7. Atsdr. 2008.Toxicological profile for phenol. Division of toxicology and environmental medicine/applied toxicology branch US Department of health and human services. Georgia, United States, 1–20.

8. Bocos, E., Iglesias, O., Pazos, M., Ángeles Sanromán, M. 2016. Nickel foam a suitable alternative to increase the generation of Fenton's reagents. Process Safety and Environmental Protection, 101, 34–44.

9. Bury, N.A., Mumford, K.A., Stevens, G.W. 2021. The electro-Fenton regeneration of Granular Activated Carbons: Degradation of organic contaminants and the relationship to the carbon surface. Journal of Hazardous Materials, 416.

10. Dao, K.C., Yang, C.C., Chen, K.F., Tsai, Y.P. 2020. Recent trends in removal pharmaceuticals and personal care products by electrochemical oxidation and combined systems. Water (Switzerland), 12(4).

11. Davarnejad, R., Sahraei, A. 2016. Industrial wastewater treatment using an electrochemical technique: an optimized process. Desalination and Water Treatment, 57(21), 9622–9634.

12. Fahem, A.S., Abbar, A.H. 2020. Treatment of petroleum refinery wastewater by electro-Fenton process using porous graphite electrodes. Egyptian Journal of Chemistry, 63(12), 4805–4819.

13. Fockedey, E., Lierde, A. Van 2002. Coupling of anodic and cathodic reactions for phenol electro-oxidation using three-dimensional electrodes, 36, 4169–4175.

14. Ghjair, A., Abbar, A. 2022. Removal of chemical oxygen demand (COD) from hospital wastewater by electro fenton process using graphite–graphite electrochemical system. Al-Qadisiyah Journal for Engineering Sciences, 15(1), 23–31.

15. Gümüş, D., Akbal, F. 2016. Comparison of Fenton and electro-Fenton processes for oxidation of phenol. Process Safety and Environmental Protection, 103, 252–258.

16. Haji Ali, B., Baghdadi, M., Torabian, A. 2021. Application of nickel foam as an effective electrode for the electrochemical treatment of liquid hazardous wastes of COD analysis containing mercury, silver, and chromium (VI). Environmental Technology and Innovation, 23.

17. He, H., Zhou, Z. 2017. Electro-fenton process for water and wastewater treatment. Critical Reviews in Environmental Science and Technology, 47(21), 2100–2131.

18. Ho, S. 2022. Low-Cost Adsorbents for the Removal of Phenol/Phenolics, Pesticides, and Dyes from Wastewater Systems: A Review. Water (Switzerland), 14(20).

19. Hu, X., Tian, X., Lin, Y.W., Wang, Z. 2019. Nickel foam and stainless steel mesh as electrocatalysts for hydrogen evolution reaction, oxygen evolution reaction and overall water splitting in alkaline media. RSC Advances, 9(54), 31563–31571.

20. Ibrahim, M.H., Salman, R.H. 2022. Study the Optimization of Petroleum Refinery Wastewater Treatment by Successive Electrocoagulation and Electrooxidation Systems. Iraqi Journal of Chemical and Petroleum Engineering, 23(1), 31–41.

21. Issa, Z.M., Salman, R.H. 2023. Chromium Ions Removal by Capacitive Deionization Process: Optimization of the Operating Parameters with Response Surface Methodology. Journal of Ecological Engineering, 24(1), 51–65.

22. Khalid, M.W., Salman, S.D. Adsorption of Heavy Metals from Aqueous Solution onto Sawdust Activated Carbon. Journal Al-Khwarizmi Engineering Journal, 15(3), 60–69.

23. Li, Q., Gao, X., Liu, Y., Wang, G., Li, Y.Y., Sano, D., Wang, X., Chen, R. 2021. Biochar and GAC intensify anaerobic phenol degradation via distinctive adsorption and conductive properties. Journal of Hazardous Materials, 405(August), 124183.

24. Lütke, S.F., Igansi, A.V., Pegoraro, L., Dotto, G.L., Pinto, L.A.A., Cadaval, T.R.S. 2019. Preparation of activated carbon from black wattle bark waste and its application for phenol adsorption. Journal of Environmental Chemical Engineering, 7(5).

25. Mohd, A. 2022. Presence of phenol in wastewater effluent and its removal: an overview. International Journal of Environmental Analytical Chemistry, 102(6), 1362–1384.

26. Nidheesh, P.V., Ganiyu, S.O., Martínez-Huitle, C.A., Mousset, E., Olvera-Vargas, H., Trellu, C., Zhou, M., Oturan, M.A. 2023. Recent advances in electro-Fenton process and its emerging applications. Critical Reviews in Environmental Science and Technology, 53(8), 887–913.

27. Norra, G.F., Radjenovic, J. 2021. Removal of persistent organic contaminants from wastewater using a hybrid electrochemical-granular activated carbon (GAC) system. Journal of Hazardous Materials, 415(February), 125557.

28. Oturan, N., Bo, J., Trellu, C., Oturan, M.A. 2021. Comparative Performance of Ten Electrodes in Electro-Fenton Process for Removal of Organic Pollutants from Water. ChemElectroChem, 8(17), 3294–3303.

29. Roddaeng, S., Promvonge, P., Anuwattana, R. 2018. Behaviors of hydrogen sulfide removal using granular activated carbon and modified granular activated carbon. In MATEC Web of Conferences. EDP Sciences, 192.

30. Siburian, R., Sihotang, H., Lumban Raja, S., Supeno, M., Simanjuntak, C. 2018. New route to synthesize of graphene nano sheets. Oriental Journal of Chemistry, 34(1), 182–187.

31. Singh, S., Mahesh, S., Sahana, M. 2019. Three-dimensional batch electrochemical coagulation (ECC) of health care facility wastewater—clean water reclamation. Environmental Science and Pollution Research, 26(13), 12813–12827.

32. Sun, Y., Li, P., Zheng, H., Zhao, C., Xiao, X., Xu, Y., Sun, W., Wu, H., Ren, M. 2017. Electrochemical

treatment of chloramphenicol using Ti-Sn/γ-Al2O3 particle electrodes with a three-dimensional reactor. Chemical Engineering Journal, 308, 1233–1242.

33. Umar, S., Bakhary, N., Abidin, A.R.Z. 2018. Response surface methodology for damage detection using frequency and mode shape. Measurement: Journal of the International Measurement Confederation, 115, 258–268.

34. Wan, W., Zhang, Y., Ji, R., Wang, B., He, F. 2017. Metal Foam-Based Fenton-Like Process by Aeration. ACS Omega, 2(9), 6104–6111.

35. Yan, L., Ma, H., Wang, B., Wang, Y., Chen, Y. 2011. Electrochemical treatment of petroleum refinery wastewater with three-dimensional multi-phase electrode. Desalination, 276(1–3), 397–402.

36. Yang, B., Tang, J. 2018. Electrochemical oxidation treatment of wastewater using activated carbon electrode. International Journal of Electrochemical Science, 13(1), 1096–1104.

37. Yang, C., Liu, H., Luo, S., Chen, X., He, H. 2012. Performance of Modified Electro-Fenton Process for Phenol Degradation Using Bipolar Graphite Electrodes and Activated Carbon. Journal of Environmental Engineering, 138(6), 613–619.

38. Zhang, C., Jiang, Y., Li, Y., Hu, Z., Zhou, L., Zhou, M. 2013. Three-dimensional electrochemical process for wastewater treatment: A general review. Chemical Engineering Journal, 228, 455–467.

39. Zhang, Y., Chen, Z., Wu, P., Duan, Y., Zhou, L., Lai, Y., Wang, F., Li, S. 2020. Three-dimensional heterogeneous Electro-Fenton system with a novel catalytic particle electrode for Bisphenol A removal. Journal of Hazardous Materials, 393.

40. Zheng, Y., Qiu, S., Deng, F., Zhu, Y., Li, G., Ma, F. 2019. Three-dimensional electro-Fenton system with iron foam as particle electrode for folic acid wastewater pretreatment. Separation and Purification Technology, 224, 463–474.